Creep-resistant aeroengine shaft steels: precipitates and consequences

Zixin Huang

Published online: 19 Jun 2019.

Submit your article to this journal ⬚

View Crossmark data ⬚

Iom³
The Institute of Materials,
Minerals and Mining

Taylor & Francis
Taylor & Francis Group

REVIEW

Creep-resistant aeroengine shaft steels: precipitates and consequences

Zixin Huang

Materials Science and Metallurgy, University of Cambridge, Cambridge, UK

ABSTRACT
Creep resistant steels must be stable over long periods of time under severe operating conditions. This paper reviews precipitation in Cr–Mo steels and maraging steels destined for elevated temperature applications. It also covers aspects of structural evolution, strengthening and degradation, all of which are essential for alloy design. Two classes of steels are emphasised, those with origins in the power generation industries, and a novel approach based on intermetallic precipitates.

Introduction

There is a need for stronger aeroengine shaft steels to enable novel engine designs. Steel shafts in the design are required to operate over a temperature range from 150°C to 450°C where creep resistance, toughness and microstructural stability become important [1]. An improved shaft would help reduce the engine core diameter, engine weight, with a high bypass ratio and enable high bypass ratio leading to greater propulsive efficiency [2]. Precipitates have an important role in the achievement of good creep properties. This review covers common precipitates and their effects in creep-resistant steels, in particular, Cr–Mo steels and maraging alloys (Table 1) .

Current shaft materials

The traditional shaft material is 'Super-CMV' (low alloy Cr–Mo steel), which has good temperature stability but insufficient strength, ductility and fracture toughness for future engine designs [4]. It also has to be inertia friction welded to AerMet 100 (Ni–Co tempered martensitic steel) for the composite to meet the toughness requirements at the lower temp end of the whole shaft [5], providing the temperature stability at the curvic coupling and the strength at the spline [6]. The mechanical properties of Super-CMV and AerMet 100 are listed in Table 2. With appropriate heat treatment, AerMet 100 has a yield strength of 1756 MPa and fracture toughness of 170 MPa $m^{1/2}$ due to the nano-scale Mo-rich M_2C [3,8]. Although AerMet 100 is used as part of the shaft, it is not a creep resistant alloy and does not have microstructural stability if tempered above 480°C because of unstable reverted austen- ite formation and precipitation coarsening, resulting in loss in toughness and strength, respectively [9]. The nature of the inertia friction welding process generates a heat-affected zone with metastable martensite and retained austenite in Super-CMV and retained austenite in AerMet 100, which must be eliminated through heat treatment [3].

Design criteria

The shaft needs to be suitable for the use in the temperature range 150–450°C. Based on current shafts, the novel shaft material must combine the mechanical properties of Super-CMV and AerMet 100 in a single alloy, which requires an excellent combination of strength, ductility, toughness, thermal stability and creep resistance so that it can serve in the temperature gradients expected during service in an aircraft engine as listed in Table 3 [5]. The required ultimate tensile strength is approximately 1900 MPa at 20°C and 1150 MPa at 450°C. The creep properties of Super-CMV are acceptable, however, the aim is to achieve strength similar to that of Super-CMV at 450°C for the designed alloy at 480°C with 0.2% or 0.5% total plastic strain [10]. During service, high cycle fatigue from the torque transfer to the shaft and engine (over 10^5 cycles before failure) is required under conditions of $R = 0$ ($R = \sigma_{min}/\sigma_{max}$). High purity and good surface finish are desirable for better fatigue properties. It also needs to be able to operate at 450°C for more than 3000 h, without the occurrence of dislocation creep [7]. In addition, microstructural stability and mechanical stability over the service life are required.

CONTACT Zixin Huang zh280@cam.ac.uk Materials Science and Metallurgy, University of Cambridge, 27 Charles Babbage Road, Cambridge CB3 0FS, UK

Table 1. Composition of AerMet 100 and Super-CMV (wt-%) [3].

Alloy	C	Ni	Co	Cr	Mo	Mn	V	Si
AerMet 100	0.23	11.10	13.40	3.00	1.20	–	–	–
Super-CMV	0.39	< 0.30	–	3.25	0.95	0.55	0.20	0.23

Table 2. Mechanical property of Super-CMV and AerMet 100 ('fatigue' is the maximum stress at $R = 0$ ($R = \sigma_{min}/\sigma_{max}$) to give a fatigue life of 10^5 cycles) [7].

Property	Temperature/°C	AerMet 100	Super-CMV
Yield strength (Y_S)	450	1280 MPa	1030 MPa
Ultimate tensile strength (UTS)	450	1561 MPa	1330 MPa
Elongation	25–450	12–18%	12–16%
Creep	450	–	857 MPa
'Fatigue' parameters	25	1400 MPa	–
'Fatigue' parameters	450	1079 MPa	875 MPa

Table 3. Mechanical property requirements of the novel shaft ('fatigue' is the maximum stress at $R = 0$ ($R = \sigma_{min}/\sigma_{max}$) to give a fatigue life of 10^5 cycles) [4,7].

Property	Temperature (°C)	Required standard
Yield strength (Y_S)	20	1350 MPa
Yield strength (Y_S)	400	1100 MPa
Ultimate tensile strength (UTS)	20	1900 MPa
Ultimate tensile strength (UTS)	400	1650 MPa
Elongation	25–450	6%
Charpy impact energy	20	12 J
Fracture toughness	20	50 MPa$\sqrt{m}$
Creep	450	857
'Fatigue' parameters	20	1350 MPa
'Fatigue' parameters	450	1050 MPa

Cr–Mo steels

Chromium–molybdenum (CrMo) and chromium–molybdenum–vanadium (CrMoV) alloys are intended mostly for high temperature (350–600°C) service. These alloys are expected to have a service life at least for 25,000 h [11]. Owing to their excellent combination of tensile strength, corrosion resistance and creep resistance at high temperatures and high pressure, the alloys have a good strength to weight ratio, allowing the use of smaller diameter shafts to reduce the overall weight. Higher creep strength can be achieved by adding solutes such as Mo, W, V, Nb [12], but to use the Cr–Mo alloy in aeroengine shafts, necessitate a high fracture toughness, low ductile-to-brittle transition temperature and significant creep resistance. Meanwhile, microstructural degradation needs to be minimised to achieve higher service temperature. Therefore, the carbide formed during tempering must be resistant to coarsening.

Microstructure

There is a wide range of heat resistant Cr–Mo alloys and most have sufficient solute concentrations to generate a martensitic microstructure with a high density of dislocations (Table 4). Then, the steels are tempered to form a stable microstructure containing various alloy carbides precipitated in the matrix, and the martensite

Table 4. Typical compositions of various Cr–Mo steel (wt-%) [13].

	C	Cr	Mn	Ni	Mo	W	V	Nb	B	N
X20	0.2	11.5	–	0.7	1	–	0.25	–	–	–
P91	0.1	9	–	0.1	0.5	–	0.2	0.06	0.002	0.05
P92	0.11	8.96	0.46	0.06	0.47	1.84	0.2	0.07	0.001	0.05
G92 [14]	0.1	9.2	0.44	–	0.45	1.82	–	–	–	–

laths acquire a subgrain structure [15]. Various intermetallic compounds have been found in Cr–Mo alloy, including Laves phase, in addition to carbides/nitrides such as $M_{23}C_6$ and minor phases as spherical NbC, fine needle-like V(C,N), M_6C (M = metal) etc. [12]. Its microstructure can be changed by thermal or mechanical processes [16], therefore gradual microstructural degradation may take place during service in creep conditions, resulting in reduced properties. Furthermore, the nucleation and coarsening of precipitates during service are detrimental to the microstructure, resulting in the final creep failure.
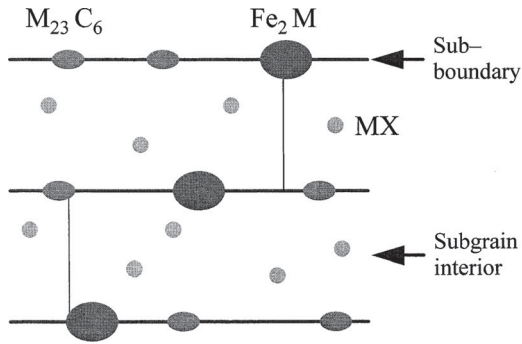
MX precipitates

'MX' represents a compound of metal atoms with X = C or N. In the presence of strong carbide or nitride forming elements (Nb, V, Ti, Zr, Ta, etc.), the formation of MX is helpful in enhancing long-term creep resistance. A typical heat treatment involves austenitisation between 1100°C and 1250°C for 30–60 min conducted normally before service to dissolve as much as MX possible [17]. Subsequent fine precipitation is beneficial in retarding creep. There are four types of MX here, coarse NbX that remains after normalising, fine spherical NbX and platelike VX that form during tempering, and VX 'wings' formed on fine NbX particles during tempering [18].

The MX carbonitride has a NaCl face-centred cubic lattice, and precipitates mainly in the matrix within laths and some along boundaries (Figure 1). The creep property of steel is highly dependent on the solubility of MX and proportion of each element that add. Kikuchi et al. [20] proposed that excessive additions of M and X lead to coarse MX and rapid coarsening of later precipitated MX. However, this does not apply before the solubility limit is reached.

$M_{23}C_6$

'$M_{23}C_6$' is a general notation for $Cr_{23}C_6$ where the Cr is partially substituted by Ni, Mo and Fe. It has a fcc lattice, and precipitates in the vicinity of grain boundaries, sub-grain boundaries and also within austenite grain. It can form in 30 min at 750°C in high chromium steel [21]. These precipitates are usually coarse ($\sim$ 200 nm in size) with a comparatively high coarsening rate and detrimental to mechanical properties, especially creep strength [17]. With the addition of small amounts of boron, the coarsening rate of $M_{23}C_6$ is reduced, thus the

Figure 1. Illustration of precipitation in high Cr ferritic steel after Maruyama [19].

number density of $M_{23}C_6$ along the grain boundaries increases, impeding grain boundary sliding [19].

Beckitt and Clarck [22] have found that $M_{23}C_6$ also grow on dislocations, and form continuous chains and clusters. $M_{23}C_6$ can stimulate dislocation emission, while providing the nucleation sites for further precipitation. Salsmal [23] have also found $M_{23}C_6$ plates form around undissolved $Nb(C,N)$ in 16Cr–16Ni–0.8Nb steel, perhaps due to the strain around the undissolved particles.

M_6C

M_6C has a wide composition range, and forms at long aging times. The composition of M_6C in steel can be Fe_3Nb_3C or Fe_3Mo_3C. Honeycombe [24] has proposed that prolonged tempering at 700°C leads to the massive formation of M_6C particles on the grain boundaries which replaces M_2C. This results in softening of the steel, which is not desirable for creep resistant steel. However, the addition of vanadium is able to stabilise Mo_2C [25].

Laves phase

Laves phase is an intermetallic compound, with the general formula A_2B ($A = $ Fe, Cr, $B = $ Mo, W, Nb) [26]. It normally is found in steel containing 2 Mo wt-% and 9–12 Cr wt-%, where the introduction of Cr increases its temperature stability [27]. In common alloys, Laves phase is thermodynamically stable between 600°C and 750°C [7], which is higher than the service temperature of aerospace shafts ($< 450°C$).

There is debate on the effect of Laves phase on the long-term creep strength; its precipitation depletes the Mo and W concentrations in the matrix, which can lead to a reduction on the creep strength if the Laves phase precipitates are coarse with a low number density [28]. However, Laves phase precipitates have been found to contribute to creep strength by precipitation hardening under certain circumstances recently [28].

Lee et al. [14] have reported the size of Laves phase of ~ 80 nm in diameter after exposure at 600°C for more than 300 h in Grade 92 steel (Table 4). He also found creep strength dropped when Laves phase reached an

average diameter of 130 nm where the formation of cavity at Laves phase triggers the brittle intergranular fracture. Exposure at 600°C for 5000–10,000 h also leaves a particle size of 280 nm in P92 steel [29].

Strengthening mechanisms

There are three main strengthening mechanisms in the heat resistant Cr–Mo steel that are active under the circumstances of shaft applications:

Solution strengthening

W and Mo in solid solution improve the creep strength of martensite [30]. As shown in Figure 2 [31], the creep rate of α-Fe is reduced by two orders of magnitude by the addition of 2.3 wt-% W in a binary Fe-W alloy. The α-Fe is free of particles, subgrain structures and free dislocations so these data represent a controlled experiment. The magnitude of the benefit is, however, small when there is an overwhelming constitution.

Precipitate strengthening

The addition of alloying elements enhances the creep strength either by being dissolved in the matrix and
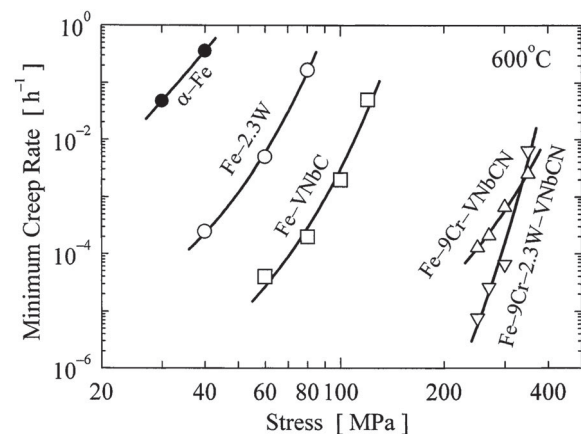
Figure 2. Minimum creep rate of α-Fe and ferritic steels at 600°C (mass%) [31].
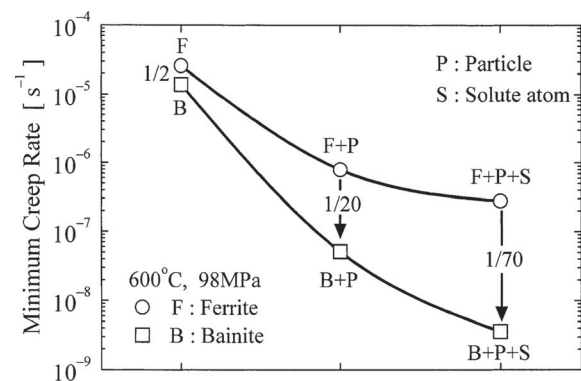
Figure 3. Minimum creep rate of ferritic (F) and banitic (B) steels at 600°C. +P and +S represent the addition of MX particles and solute atoms (0.6 W + 0.15 Mo in wt-%) to the steels [38].

Table 5. Role of elements in Cr–Mo steel [19,41].

Element	Advantage	Disadvantage
B	Improve creep resistance and hardenability; Stabilise $M_{23}C_6$ and retard its coarsening	Decrease impact toughness
C	Necessary to form $M_{23}C_6$ and NbC	Lowers ductility, toughness and machinability.
N	Necessary to form VN	Increase brittleness, reduce weldability
Cr	Improve oxidation resistance; form $M_{23}C_6$, lower M_s.	Increase diffusivity
Nb	Suppress δ-ferrite, decrease diffusivity.	Reduce hardenability, impact toughness and elongation; raise M_s
Cu	Increase atmospheric corrosion resistance	Promote precipitation of Laves phase
Mo	Reduce temper brittleness, lower M_s	Accelerate $M_{23}C_6$ growth
Nb	Form NbC and contribute to strengthening	Promote precipitation of Z-phase (CrXN, where X = Nb, V or Ta)
Mn	Improve forgeability, lower M_s.	Reduce plasticity and weldability, promote M_6C
Ni	Improve plasticity, lower M_s.	Increase diffusivity.
Re	Eliminate MnS for purification.	–
Si	Improve oxidation resistance.	Reduce plasticity and toughness
V	Form VC and contribute to strengthening	Reduce hardenability
W	Retards $M_{23}C_6$ coarsening; solid solution strengthening, lower M_s	–
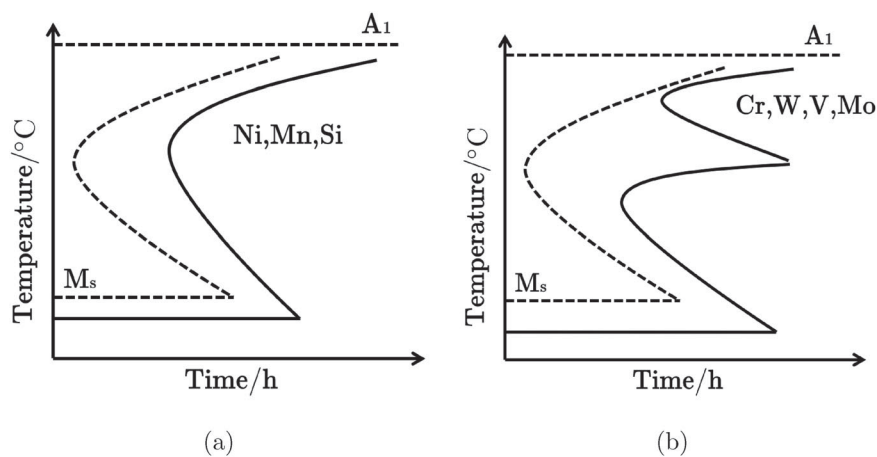
Figure 4. Time–temperature–transformation diagrams of austenite to ferrite isothermal transformation (a) carbon steel and steel alloyed with weak or non-carbide forming elements; (b) carbon steel and steel alloyed with strong carbide forming elements, after Maalekian [46].
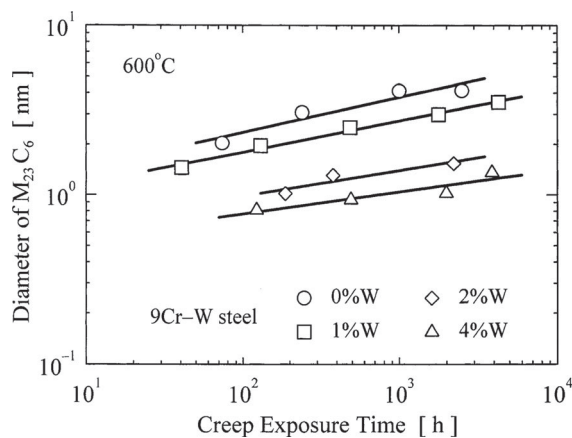
Figure 5. Effect of W on the growth of $M_{23}C_6$ particles during creep of 9Cr–1W wt-% steel at 600°C [19].

precipitates as fine carbides (NbC, Mo_2C, $M_{23}C_6$) or intermetallic (β-NiAl, Laves phase) [32]. NbC and VC particles remain the most stable in terms of their resistance to coarsening [33]. As shown in Figure 2, they reduce the creep rate tremendously in Fe-VNbC (mass%) compared with α-Fe [31] by hindering dislocation movement and retarding dislocation recovery [34]. Fine $M_{23}C_6$ is also effective in this respect, by slowing down the recovery of dislocation structure while its coarsening during creep results in acceleration of creep deformation [35]. This is also consistent with Mikami [36] who reported a condensation and coarsening of precipitates accelerating the degradation. The increase in creep resistance due to fine Fe_2M has been reported by Igarashi [37]. The thermal stability of precipitates at elevated temperature is important in resisting grain growth and slowing down dislocation recovery; thus enhancing long-term creep strength.

Dislocation strengthening

A comparison between the creep rate of ferrite (F) without dislocation substructure and banite (B) with dislocation substructure is shown in Figure 3 [38]. Th bainite has a similar dislocation substructure to tempered martensite [19]. The contribution of particles, solute
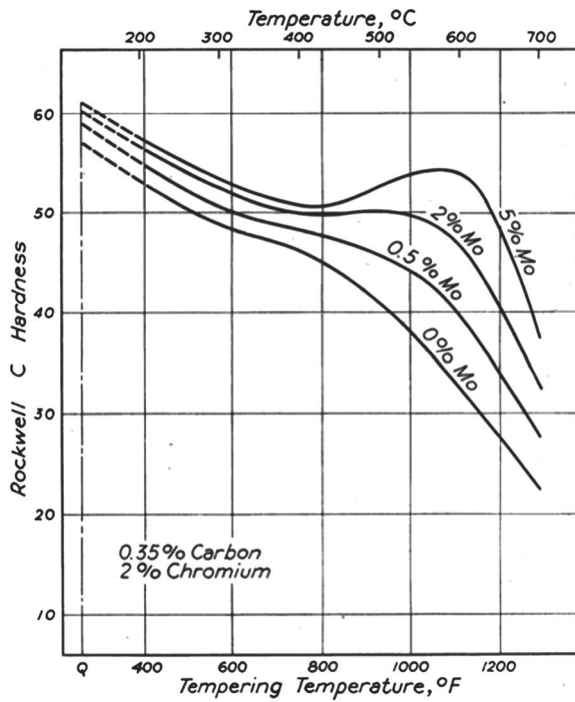
Fig. 159—The Softening, with Increasing Tempering Tempera-
ture, of 2.0 Per Cent Chromium, 0.35 Per Cent Carbon Steels as
Influenced by Molybdenum Content. (See Footnote 46).

Figure 6. The effect of molybdenum on the tempering of
quenched steel Fe–0.35C–2Cr wt-% [53].

atoms and dislocations lower the creep rate. However,
the dislocation substructure is not effective without the
introduction of particles and solute atoms.

Steel with a smaller subgrain size has better creep
than one with a coarser [19]. In the same study, 11 Cr
steel tempered at 680°C has a much higher disloca-
tion density than tempered at 780°C, suggests the dis-
location density increases with decreasing tempering
temperature. Notably, the former one reaches 1% strain
at 70% rupture life, and latter at 10% of rupture life,
even with the same subgrain size. It can be concluded
that the large free dislocation density as well as fine
subgrain size both contribute to better creep resistance
[39]. Moreover, Endo et al. also have reported that the
reduced dislocation density and lath boundaries move-
ment are responsible for about 65% loss of hardness
in 9Cr–1Mo wt-% steel during creep in the range of
stress and temperature from 71 to 167 MPa and 600 to
650°C [40].

Effect of alloying elements

The effects of alloying elements have been summarised
in Table 5.

- *Carbon and nitrogen:* For steels with up to 0.2
  wt-% carbon, approximately 90% of carbon seg-
  regates to the dislocations and lath boundaries
  during quenching. During tempering, the carbon
  precipitates, contributing to the overall strength.
  However, it can reduce toughness, weldability, cor-
  rosion resistance and by making carbides more
  stable can make it difficult to dissolve them during
  austenitisation [42].
  Nitrogen also strengthens by precipitation as
  nitride of Ti or Nb. However, nitrogen in solid
  solution is much more effective at strengthening
  than carbon [17]. It retards the nucleation and
  coarsening of $M_{23}C_6$ due to its low solubility in this
  carbide [43–45].
- *Alloying elements:* Figure 4 shows that solutes such
  as Mn, Mo, W delay the transformation to ferrite
  and pearlite so that martensite can be generated
  at relatively low cooling rates. They also reduce
  the martensite-start temperature, giving a fine sub-
  grain structure.
  Besides enhanced hardenability, wear resistance,
  corrosion resistance, impact resistance and machin-
  ability, Cr and Mo improve the creep properties by
  precipitation strengthening [19]. They also facili-
  tate carbide precipitation and promote the forma-
  tion of Laves phase on long-term aging. As shown
  in Figure 5, the addition of W delays the coarsen-
  ing of $M_{23}C_6$ [47] and the addition of a very small
  amount of boron has a similar effect [48–50]. Both
  of these solutes do not influence MX coarsening
  [51,52]. As strong carbide formers, Nb, Ti and V
  improve the creep strength by precipitating car-
  bides, nitrides or carbo-nitrides which are stable
  and do not coarsen during service [17].

Secondary hardening

Secondary hardening in a series of steels with increas-
ing molybdenum content at around 600°C is illustrated
in Figure 6 [53]. Needle-shaped Mo_2C about 100–200 Å
long and 10–20 Å in diameter at peak hardness in

Table 6. Comparison of W_2C and Mo_2C dispersion at peak hardness (tempering at 550°C)
[54].

| Alloy (at-%) | Time to peak hardness (h) | Peak hardness (HV) | Precipitate dispersion | | Density (cm^{-3}) |
| | | | Size(Å) | | |
			Diameter	Length	
Fe–2W–1C	20	410	23–35	200–300	1×10^{16}
Fe–2Mo–1C	15	515	15–25	100–200	2–4×10^{17}

Fe–2Mo–1C (at-%) [54], growing along $<100>$ direction in ferrite. Tungsten produces similar secondary hardening carbides (Table 6), but the formation of W_2C is slower because of the smaller diffusivity of tungsten in ferrite relative to that of molybdenum.

Secondary hardening is more effective with strong carbide formers such as Nb, Ti, V, which enhances the peak hardness and resist overaging. Raynor et al. [25] found that 0.06 Nb at-% or Ti to Fe–3.6 Mo–0.2C wt-% increases the peak hardness by approximately 20 HV at $563°C$,and retards overaging. The introduction of 0.5 V wt-% to Fe–2.5 Mo–0.2C wt-% is more effective in this context because of the fine precipitation of a large amount of V_4C_3 and its influence on the coarsening of Mo_2C.

Without forming carbide, cobalt it has a similar effect by limiting dislocation recovery during tempering, which provides more nucleation sites for precipitates [55,56]. It also increases carbon diffusivity, promoting fine precipitate formation [57].

The replacement of coarse cementite by fine (Mo, Cr)$_2$C enhances toughness during tempering [55] of 10Ni–8Co–2Cr–1Mo–0.2C wt-% steels.

Maraging steels

Maraging steels are a class of low-carbon steels with Ni, Cr and other substitutional solute that may precipitate during aging [58]. On cooling, the austenite transforms into relatively soft martensite albeit with a high dislocation density, and intermetallic compounds are then induced by tempering in the range $450–550°C$. These steels are strong and tough in the absence of carbon, which makes for a wide range of applications including aerospace, military industry, tooling and machinery [59]. Typical requirements include 0.2% proof strength of 1250–1350 MPa, the tensile strength of 1500–1600 MPa, fracture toughness of $50\,MPa\sqrt{m}$ and elongation of 6% as listed in Table 3 [4].

Traditional maraging steels (Table 7) such as 18Ni grade, are categorised by their UTS (200, 250, 300, 350) [60]. The high Ni content ensures only martensitic transformation occurs even at a moderate or slow cooling rate quenching. However, martensite enriched with Ni is thermodynamically unstable at elevated temperature and reversion to austenite can occur after prolonged exposure to high temperature. In order to meet various requirements, more steels such as IRK91, 347, etc. have been developed.

Microstructure

The matrix following cooling from the austenite phase field is martensite with some austenite retained. The large concentrations of Ni, Cr and other solutes allow

Table 7. Typical compositions of various maraging steel (wt-%).

	C	Ni	Cr	Co	Mo	Nb	Mn	Si	Al	Ti	Cu
C250 [64]	–	18	–	10	5.5	–	–	–	–	0.5	–
C300 [65]	0.1	18	–	8.8	2.9	–	–	–	0.2	0.7	–
T300 [65]	0.1	18	–	–	2.4	–	–	–	0.2	2.2	–
IRK91 [63]	0.01	9	12	–	4	–	0.3	0.15	–	–	2
347 [66]	0.07	11.5	18.5	–	–	0.8	1.6	0.65	–	–	–

Table 8. Precipitate phases in maraging steels [7].

Phase	Formula
η,	$Ni_3(Ti,Al,Mo)$
γ'	$Ni_3(Al,Ti)$
γ	$Ni_3(Mo,W)$
β	$NiAl$
ϵ-Cu	Cu
G	$Ni_{16}Ti_6Si_7$
μ	$(Fe, Co, Ni)_7(Cr, Mo, W)_6$
Laves	$Fe_2(Mo,W,Ti)$
R	$(Fe,Co,Ni)CrMo$

martensitic transformation during oil cooling. A cryogenic treatment may be applied to reduce the retained austenite content [61].

The intermetallic compounds precipitate at temperatures in the range $400–500°C$, accelerated by the high dislocation density and the diffusion of substitutional solutes [62]. The precipitated intermetallic compounds in maraging steel are listed in Table 8. The critical precipitates depend on the detailed chemical composition. For applications at approximately $450–625°C$, Laves phase and β-NiAl are desirable due to their excellent high temperature stability.

Laves phase

Fine Laves phase (50 nm) has been reported [63] to impede the movement of subgrains and dislocations in IRK91 (Table 7), these continuing to precipitate strengthening, even though solid solution strengthening described as Mo, W or Cr are depleted [67,68]. W tends to accelerate the coarsening of Laves phase [69–71].

In niobium stabilised 347 steels (Table 7), Fe_2Nb forms after long aging, as a transient phase which disappears to give way to Fe_3Nb_3C. Laves phase also appears as a transition precipitates, dissolving as Fe_3Nb_3C or NbC form [66].

Similarly, unstable Ni_3Mo formed at the initial stages of aging gives way to the more stable Fe_2Mo during prolonged aging in C250 maraging steel (Table 7) [64].

β-NiAl

The β-NiAl is the main strengthening phase in Al-containing alloys with ordered B2 (CsCl) structure [72]. It typically is stable up to $700°C$ but only precipitates in the absence of Ti; this has been attributed to its tendency to form η-Ni_3Ti. β-NiAl precipitates from solute-rich clusters, and grow to be spherical at first [73], become more cuboidal as it grows, and overtime

Table 9. Matrix composition of C300 and T300 after tempering at 510°C for 8 h (wt-%).

Alloy	Fe	Ni	O	Mo	Ti
C300	77.8±0.4	18.1±0.1	2.7±0.2	1.0±0.3	0.07±0.07
T300	84.9±0.6	10.8±0.5	–	4.0±0.5	< 0.03

revert to be almost spherical again [74]. β-NiAl uniformly distributed in the matrix with coherency up to 150 nm in radius [62], and maintain its coherency at the aging temperature [75].

Austenite

The high Ni composition in maraging steels allows the precipitation of austenite above 350°C through aging by a diffusion controlled reaction [76,77]. The precipitated austenite is in the form of thin films at the martensite boundaries, and is able to resist coarsening and enhance fracture at the expense of yield strength [78,79]. As shown in Table 9, Co-free T300 tends to form Ni$_3$Ti which results in a lower matrix Ni composition [65]. A low Ni concentration in the matrix reduces the tendency to form austenite. Also, the reversion to austenite can be retarded to reducing the Ni concentration [80].

Strengthening mechanisms

The dominant strengthening factor is precipitate hardening by the intermetallic compounds [81], for example, fine Laves phase and β-NiAl in the novel maraging steel studied here [82–85].

Apart from precipitation, strong elements such as nickel have meltable sites, for example in enhancing hardenability. If nickel is formed to result in too much retained austenite, then some of it can be replaced with Cr to maintain hardenability [7]. Chromium also provides oxidation and corrosion resistance to the alloy and is effective in solid solution strengthening. Excessive chromium can promote the precipitation of δ-ferrite at higher temperatures [86].

Cobalt increases the M$_s$ temperature while maintaining the hardenability [59,87]. Tungsten and molybdenum improve the resistance to creep by solution strengthening and forming M$_2$C and Laves phase particles [30], although the latter represents a minor contribution due to the tendency for the precipitate to be coarse [88]. Aluminium is necessary for β-NiAl, 1.75 Al wt-% produces 5.0 wt-% β-NiAl at 560°C [59]. However, it raises the M$_s$ temperature, so its concentration needs to be controlled.

Nitrogen promotes coarse Ti(C,N) and AlN particles that form at very high temperatures, which initiate fatigue. Mn and P raise the hardenability but their segregation at grain boundaries can lead to embrittlement in the aged condition [89]. Therefore, N, Mn and P concentrations should be as low as possible.

Grain size and mechanical properties

The relationship between grain size and strength [90,91], ductile to brittle transition [92,93], creep [94,95] and fatigue [96,97] have been measured and modelled for steels. An austenite grain after transformation will contain packets, blocks and laths. A packet has a series of parallel laths, slightly misorientated, whereas a block consists of laths with similar orientations. Based on previous researches on the steel [98], the relationship between the block size (d) and austenite grain size d_γ is:

$$d = \eta d_\gamma{}^{1/2}, \tag{1}$$

where η is 0.3 for maraging and low carbons alloys.

Grain refinement is a traditional way to improve strength according to Hall–Petch Equation [99,100]:

$$\sigma = \sigma_0 + k_y d^{-1/2}, \tag{2}$$

where σ is yield strength, σ_0 is friction stress, (d) is grain sizes, k_y is 2190 MPa μm$^{-1/2}$ for $d = d_\gamma$ [91,101] and $\sim$ 684 HV μm$^{-1/2}$ for block size [85].

The ductile to brittle transition temperature (T$_{DBTT}$) is highly dependent on the stress required to move dislocations; fine structure is generally associated with a low T$_{DBTT}$, thus longer elongation for crack propagation [102].

A large grain size can benefit creep resistance if the dominant mechanism is grain boundary diffusion [103], but not otherwise. It has often been found that smaller grain size tends to have a lower creep rate and a longer creep life at low to intermediate temperatures (below half of the melting temperature) [94,95,104–106]. Grain boundaries would act as barriers and dislocation sources, which would impede dislocation movement [94]. This suggests additional grain refinement would be promising for improved creep performance.

Methods of grain size refinement

Grain refinement can be achieved through dispersed fine carbides, nitrides or carbo-nitrides that hinder growth at the austenitising temperature by pinning grain boundaries during hot deformation [107]. For 0.10 Nb wt-% or Ti and 0.06 C wt-%, NbC and TiC are stable up to 1200°C [46]. The vanadium nitride remains undissolved until the temperature exceeds 1000°C in steel containing 0.10 V wt-% and 0.10 N wt-% [108]. The addition of 0.005 Nb wt-% and 0.06 V wt-% has been found to reduce the prior austenite grain size (PAGS) from approximately 25 μm to 18 μm in 0.01 C–1.25Mn wt-% steel after austenitisation at 1075°C for 1 h by precipitation of fine (Nb,V)C with an average size of around 25±16 nm [109]. For Nb, a fine dispersion of nanosized NbC (2–10 nm diameter) is more effective in retarding recrystallization than dissolved Nb in the matrix. An atomic ratio of Nb/C > 1

or Nb/(C N) > 1 is found to be preferred due to the combination of precipitation strengthening and solid solution strengthening in refining prior austenite grain size[110]. This is also consistent with Kikuchi et al. [111], Adamson [112] and Keown and Pickering's study [113].

The combination addition of Nb, Ti with B is found to be more effective in retarding recrystallisation than single addition of B, Ti or Nb [114]. Tamehiro et al.[115] found that the addition of Nb to B steel not only slow down the recrystallisation but also suppress the $M_{23}(B,C)_6$ precipitation, which gives a fine structure.

Elements that are not deliberate additions, like Al, V and Ti, favour forming nitrides in austenite which may be effective in inhibiting grain growth but can be detrimental to the overall mechanical properties [116].

Concluding remarks

The application of the material is based on the application for aerospace shaft, will only tolerance for up to 0.5% creep strain. Its particular required strength level determines the particular level of precipitate strengthening needed. A uniform distribution of intermetallic compounds and stable carbides would contribute to improved creep properties. However, coarse $M_{23}C_6$ and Laves phase present at prior austenite grain boundaries, or even junctions, would result in creep voids to link together, coalescing and be detrimental to creep life. Therefore, the designed alloy need to have a compromise on the size and number of intermetallic compounds. The heat treatment must happen at a temperature above the service temperature in order to ensure some level of thermal stability.

The Super-CMV is well established, so it is not discussed further. But research on steels based on intermetallic compounds for shaft application as lead to a novel ultra-high strength maraging steel developed in Cambridge [82]. Owing to its unique combination of nanoscale Laves phase and β-NiAl, it has a balanced ductility and creep resistance. It has a yield strength above 1800 MPa, the ultimate tensile strength of approximately 2000 MPa, tensile ductility up to approximately 8% at room temperature. This alloy ticks all the right boxes with respect to the properties required exclude creep rupture life which is below 3000 h under 700 MPa at 500°C. Based on the literature, grain size refinement would be promising to enhance its creep properties.

Futuer aspects that need to be considered and researched, particularly in the context of intermetallic compounds strengthened alloys are listed below:

- Thermal stability of any material developed is an extreme requirement for aeroengine shaft applications. So not enough is understood for controlling factors for thermal stability over service conditions

of the shaft. These service conditions are much more onerous than those in the power generation industries because of far greater stresses and longer service lifetime, therefore more research needs to be done. Moreover, changes in toughness over the duration of the service life needs to be explored.
- Recording systems for any new alloys are necessary for development.
- Component level testing is required for designed alloy for the aeroengine applications.

Disclosure statement

No potential conflict of interest was reported by the author.

References

[1] Evans WJ. Basic stress loads course. Rolls-Royce plc; 2008.
[2] Wickerson J. Holistic gas turbine course. Rolls-Royce plc; 2007.
[3] Moat R, Karadge M, Preuss M, et al. Phase transformations across high strength dissimilar steel inertia friction weld. J Mater Process Technol. 2008;204:48–58.
[4] Hill P. DNS138815:Mechanical property data to meet the requirements of the CoSAP for the Trent 1000 – LP turbine shaft forging to NES000592 in AerMet 100 material to MSRR6689. 2008.
[5] Guo Z. The limit of strength and toughness of steel. Lawrence Berkeley National Laboratory; 2001.
[6] Robotham WS, Hyde TH, Williams EJ, et al. Mechanical testing of dual alloy inertia friction welded shafts. Appl Mech Mater, Vol. 3, p. 131–140. Trans Tech, 2005.
[7] Barrow A. Strong, tough and fatigue-resistant steel for elevated temperature applications [PhD thesis]. University of Cambridge; 2009.
[8] Ayer R, Machmeier PM. Transmission electron micro scopy examination of hardening and toughening phenomena in aermet 100. Metall Trans A. 1993;24(9): 1943–1955.
[9] Ayer R, Machmeier PM. Transmission electron micro scopy examination of hardening and toughness phenomena in Aermet 100. Metall Trans A. 1993;24: 1943–1955.
[10] Rolls-Royce. DNS158359; 2011.
[11] Kumšlytis V, Skindaras R, Valiulis AV. The structure and properties of 5%Cr-0.5%Mo steel welded joints after natural ageing and post-weld heat treatment. Mater Sci. 2012;18:119–122.
[12] Kim SH, Ryu WS, Kuk IH. Microstructure and mechanical properties of Cr-Mo steels for nuclear industry applications. Nucl Eng Tech. 1999;31:561–571.
[13] Danielsen HK. Z-phase in 9–12% Cr steels [PhD thesis], Department of Manufacturing, Engineering and Management, Technical University of Denmark; 2007.
[14] Lee JS, Armaki HG, Maruyama K, et al. Causes of breakdown of creep strength in 9Cr-1.8W-0.5Mo-VNb steel. Mater Sci Eng A. 2006;428(1–2):270–275.
[15] Eggeler G, Nilsvang N, Ilschner B. Microstructural changes in a 12% chromium steel during creep. Steel Res. 1987;58(2):97–103.
[16] Micheľ J, Buršák M, Vojtko M. Microstructure and mechanical properties degradation of crmo creep resistant steel operating under creep conditions. Materials Engineering-Materialove inzinierstvo (MEMI). 1:57–62.

[17] Sourmail T. Precipitation in creep resistant austenitic stainless steels. Mater Sci Technol. 2001;17: 1–14.

[18] Ennis PJ, Zielinska-Lipiec A, Wachter O, et al. Microstructural stability and creep rupture strength of the martensitic steel P92 for advanced power plant. Acta Mater. 1997;45:4901–4907.

[19] Maruyama K, Sawada K, Koike J. Strengthening mechanisms of creep resistant tempered martensitic steel. ISIJ Int. 2001;41:641–653.

[20] Kikuchi M, Fujita T. International conference on creep. Japan Society of Mechanical Engineers, p. 215.

[21] Lewis MH, Hattersley B. Precipitation of $M_{23}C_6$ in austenitic steels. Acta Metall. 1965;13:1159–1168.

[22] Beckitt FR, Clark BR. The shape and mechanism of formation of m23c6 carbide in austenite. Acta Metall. 1967;15(1):113–129.

[23] Sasmal B. Mechanism of the formation of $m_{23}c_6$ plates around undissolved nbc particles in a stabilized austenitic stainless steel. J Mater Sci. 1997;32(20): 5439–5444.

[24] Honeycombe RWK. Structure and strength of alloy steels. Climax Molybdenum; 1973.

[25] Raynor D. Secondary hardening and carbide precipitation in some pure steels [PhD thesis]. University of Sheffield; 1967.

[26] Tarasenko LV, Titov VI. Processes of phase instability in high-temperature steels subjected to long-term heating. Met Sci Heat Treat. 2005;47:538–543.

[27] Sha W, Cerezo A, Smith GDW. Phase chemistry and precipitation reactions in maraging steels: part IV. Discussion and conclusions. Metall Trans A. 1993;24:1251–1256.

[28] Cui H, Sun F, Chen K, et al. Precipitation behavior of Laves phase in 10%Cr steel x12CrMoWVNbN10-1-1 during short-term creep exposure. Mater Sci Eng A. 2010;527(29–30):7505–7509.

[29] Hattestrand M, Andren HO. Microstructural development during ageing of an 11% chromium steel alloyed with copper. Mater Sci Eng A. 2001;318:94–101.

[30] Iwanaga K, Tsuchiyama T, Takaki S. Strengthening mechanisms in heat-resistant martensitic 9Cr steels. Key Engineering Materials, Vol. 171, p. 477–482. Trans Tech Publ, 2000.

[31] Kadoya Y, Shimizu E. Effect of solute Mo, W and dispersoid carbonitride on high temperature creep of ferritic steels. Tetsu-to-Hagane (J Iron Steel Inst Japan). 1999;85:827–834.

[32] Igarashi M, Sawaragi Y. Proc. Int. Conf. on power engineering-97. 1997:107.

[33] Hofer P, Cerjak H, Warbichler P. Materials for advanced power engineering 1998. In: Lecomte-Beckers J, et al. editor. Vol. Forschungszentrum Julich GmbH. Julich; 1998.

[34] Lecomte-Beckers J, Carton M, Schubert F, Ennis PJJ. Materials for advanced power engineering 2002. Forschungszentrum Jülich, Jülich, Germany, 164, 2002.

[35] Iwanaga K, Tsuchiyama T, Takaki S. Relationship between creep behavior and microstructure in martensitic heat resistant steel. Tetsu-to-Hagane (J Iron Steel Inst Jpn). 1998;84:896–901.

[36] Mikami M. Effects of dislocation substructure on creep deformation behavior in 0.2%C-9% Cr steel. ISIJ Int. 2016;56:1840–1846.

[37] Igarashi M, Sawaragi Y. Rept. of 123 Com. on heat-resisting metals and alloys. JSPS. 1994;35:285.

[38] Nishimura N, Ozaki M, Maruyama F. Key Eng. Mater. 2000;171–174:297.

[39] Iseda A, Teranishi H, Masuyama F. Effects of chemical compositions and heat treatments on creep rupture strength of 12 wt% chromium heat resistant steels for boiler. Tetsu-to-Hagané. 1990;76(7):1076–1083.

[40] Endo T, Masuyama F, Park KS. Change in vickers hardness and substructure during creep of a mod. 9cr-1mo steel. Mater Trans. 2003;44(2):239–246.

[41] Andrews KW. Empirical formulae for the calculation of some transformation temperatures. J Iron Steel Inst. 1965;203:721–727.

[42] Pickering FB. Microstructural development and stability in high chromium ferritic power plant steels, chapter Historical development and microstructure of high chromium ferritic steels for high temperature applications. Woodhead; 1997.

[43] Pickering FB. Physical metallurgical development of stainless steels. Stainless Steels, p. 2–28, London: The Institute of Metals; 1985.

[44] Marshall P. Austenitic stainless steels: microstructure and mechanical properties. Essex: Springer Science & Business Media; 1984.

[45] Berns H, Gavriljuk VG. High nitrogen steels. Berlin: Springer-Verlag; 1999.

[46] Maalekian M. The effects of alloying elements on steels (I). Institut fur Werkstoffkunde. Technische Universitat Graz, p. 36, 2007.

[47] Abe F. Coarsening behavior of martensite laths intempered martensitic 9Cr-W steels during creep deformation. Proceeding Fourth International Conference on Recrystallisation and Related Phenomena, p. 289–294, 1999.

[48] Takahashi N, Fujita T, Yamada T. Effect of boron on long period creep rupture strength of 12%Cr heat resisting steel. Tetsu-to-Hagane. 1975;61(9): 2263–2273.

[49] Lundin L, Andren HO. Atom-probe investigation of a creep resistant 12% chromium steel. Surf Sci. 1992;266(1–3):397–401.

[50] Nowakowski P, Nowakowski P, Spiradek K, et al. Microstructural basis for the high creep resistance of new 9% Cr steels modified with boron and cobalt. Fortschritte in der Metallographie, p. 89–96, 1998.

[51] Kadoya Y. Rept. of 123 com. on heat-resisting metals and alloys. JSPS. 1998;39:347.

[52] Strang A, Vodarek V. Z-phase formation in a martensitic 12CrMoVNb steel. Mater Sci Technol. 1996;12: 552–556.

[53] Irvine KJ, Pickering FB. The tempering characteristics of low-carbon low-alloy steels. J Iron Steel Inst. 1960;194:137–153.

[54] Whiteman JA, Raynor D, Honeycombe RWK. JISI. 204(349), 1966.

[55] Speich GR, Leslie WC. Tempering of steel. Metall Trans. 1972;3:1043–1054.

[56] Chandhok VK, Hirth JP, Dulis EJ. Effect of cobalt on tempering tool and alloy steels. Trans ASM. 1963;56:677.

[57] Chandhok VK, Hirth JP, Dulis EJ. Effect of cobalt on carbon activity and diffusivity in steel. Trans Metall Soc AIME. 1962;224:858.

[58] Schober M, Schnitzer R, Leitner H. Precipitation evolution in a Ti-free and Ti-containing stainless maraging steel. Ultramicroscopy. 2009;109:553–562.

[59] Decker RF, Floreen S. Maraging steels – the first 30 years. In Wilson RK, editor. Maraging steels – recent

developments and applications, p. 1–38, Warrendale, Pennsylvania, USA; 1988. TMS-AIME.

[60] Sha W, Guo Z. Maraging steels: modelling of micro structure, properties and applications. Vol. 10. Padstow, Cornwall: Taylor and Francis; 2009.

[61] Schmidt M, Rohrbach K. Heat treating of maraging steels, heat treating. ASM Handbook, ASM Int. 1991;4:219–228.

[62] Ping DH, Ohnuma M, Hirakawa Y, et al. Microstructural evolution in 13Cr-8Ni-2.5Mo-2Al martensitic precipitation-hardened stainless steel. Mater Sci Eng A. 2005;394(1–2):285–295.

[63] Liu P, Stigenberg AH, Nilsson JO. Quasicrystalline and crystalline precipitation during isothermal tempering in a 12Cr-9Ni-4Mo maraging stainless steel. Acta Metall Mater. 1995;43:2881–2890.

[64] Moshka O, Pinkas M, Brosh E, et al. Addressing the issue of precipitates in maraging steels–unambiguous answer. Mater Sci Eng A. 2015;638:232–239.

[65] Sha W, Cerezo A, Smith GDW. Atom probe studies of early stages of precipitation reactions in maraging steels II. Ti-free model alloy and Co-free T-300 steel. Scr Metall Mater. 1992;26:523–528.

[66] Minami Y, Kimura H, Ihara Y. Microstructural changes in austenitic stainless steels during long-term aging. Mater sci tech. 1986;2(8):795–806.

[67] Korcakova L, Hald J, Somers MAJ. Quantification of Laves phase particle size in 9CrW steel. Mater Charact. 2001;47(2):111–117.

[68] Zielińska-Lipiec A, Czyrska-Filemonowicz A, Ennis PJ, et al. The influence of heat treatments on the microstructure of 9% chromium steels containing tungsten. J Mater Proc Tech. 1997;64(1–3):397–405.

[69] Hu P, Yan W, Sha W, et al. Microstructure evolution of a 10Cr heat-resistant steel during high temperature creep. J Mater Sci Technol. 2011;27:344–351.

[70] Prat O, Garcia J, Rojas D, et al. Investigations on the growth kinetics of Laves phase precipitates in 12%Cr creep-resistant steels: Experimental and dictra calculations. Acta Mater. 2010;58(18):6142–6153.

[71] Spigarelli S. Microstructure-based assessment of creep rupture strength in 9Cr steels. Inter J Pressure Vessels Piping. 2013;101:64–71.

[72] Liu ZG, Frommeyer G, Kreuss M. Atom probe FIM investigations on the intermetallic NiAl phase with B2 superlattice structure. Surf Sci. 1991;246:272–277.

[73] Leitner H, Schober M, Schnitzer R, et al. Strengthening behavior of Fe-Cr-Ni-Al-(Ti) maraging steels. Mater Sci Eng A. 2011 Jun;528(15):5264–5270.

[74] Schober M, Lerchbacher Ch, Eidenberger E, et al. Precipitation behavior of intermetallic nial particles in Fe-6 at.% Al-4 at.% Ni analyzed by SANS and 3DAP. Intermetallics. 2010;18(8):1553–1559.

[75] Leitner H, Schnitzer R, Schober M, et al. Precipitate modification in PH13-8Mo type maraging steel. Acta Mater. 2011;59(12):5012–5022.

[76] Kapoor R, Batra IS. On the α' to γ transformation in maraging (grade 350), PH 13-8 Mo and 17-4 PH steels. Mater Sci Eng A. 2004;371:324–334.

[77] Markfeld A, Rosen A. The effect of reverted austenite on the plastic deformation of maraging steel. Mater Sci Eng. 1980;46:151–157.

[78] Kim SJ, Wayman CM. Precipitation behavior and microstructural changes in maraging Fe-Ni-Mn-Ti alloys. Mater Sci Eng A. 1990;128:217–230.

[79] Khan SH, Nusair Khan A, Ali F, et al. Study of precipitation behavior at moderate temperatures in 350

[80] He Y, Yang K, Sha W, et al. Microstructure and mechanical properties of a 2000 MPa Co-free maraging steel after aging at 753 K. Metall Mater Trans A. 2004;35:2747–2755.

[81] Schnitzer R, Zinner S, Leitner H. Modeling of the yield strength of a stainless maraging steel. Scr Mater. 2010 Mar;62(5):286–289.

[82] Sun L, Simm TH, Martin TL, et al. A novel ultra-high strength maraging steel with balanced ductility and creep resistance achieved by nanoscale β-nial and Laves phase precipitates. Acta Mater. 2018;149:285–301.

[83] Simm TH, Sun L, Galvin DR. A sans and apt study of precipitate evolution and strengthening in a maraging steel. Mater Sci Eng A. 2017;702:414–424.

[84] Gray V, Galvin D, Sun L, et al. Precipitation in a novel maraging steel f1e: a study of austenitization and aging using small angle neutron scattering. Mater Charact. 2017;129:270–281.

[85] Simm TH, Sun L, Galvin DR, et al. The effect of a two-stage heat-treatment on the microstructural and mechanical properties of a maraging steel. Materials. 2017;10(12):1346.

[86] Rasul M. Thermal Power Plants-Advanced Applications; 2012.

[87] Magnee A, Drapier JM, Coutsouradis D. Cobalt-containing high-strength steels. No. INIS-MF–1971; 1974.

[88] Sello MP, Stumpf WE. Laves phase precipitation and its transformation kinetics in the ferritic stainless steel type AISI 441. Mater Sci Eng A. 2011;528:1840–1847.

[89] deSouza LFG, deSouzaBott I, Jorge JCF, et al. Micro structural analysis of a single pass 2.25% Cr–1.0% Mo steel weld metal with different manganese contents. Mater Charact. 2005;55:19–27.

[90] Petch NJ. The cleavage strength of polycrystals. J Iron Steel Inst. 1953;174:25–28.

[91] Dingley DJ, McLean D. Components of the flow stress of iron. Acta Metall. 1967 May;15(5):885–901.

[92] Petch NJ. Fracture: Proceedings of an international conference on the atomic mechanisms of fracture, Swampscott (MA), USA; 12–16 April; 1959.

[93] Sun XJ, Li ZD, Yong QL, et al. Third generation high strength low alloy steels with improved toughness. Sci China Tech Sci. 2012;55(7):1797–1805.

[94] Garofalo F. Effect of grain size on the creep behavior of an austenitic lron-base alloy. Trans AIME. 1964;230:1460–1467.

[95] Wilshire B. Some grain size effects in creep and fracture. Scripta Metall. 1970;4(5):361–366.

[96] Haddou H, Risbet M, Marichal G, et al. The effects of grain size on the cyclic deformation behaviour of polycrystalline nickel. Mater Sci Eng A. 2004;379(1–2):102–111.

[97] GW Tuffnell, DL Pasquine, JH Olson. An investigation of the fatigue behavior of 18 per cent nickel maraging steel. ASM Trans Quart. 1966;59(4):769–783.

[98] Sun L. The effects of strain path reversal on austenite grain subdivision, recrystallisation and phase transformations in microalloyed steel [PhD thesis]. University of Sheffield; 2012.

[99] Hall EO. Deformation and ageing of mild steel: III discussion of results. Proc Phys Soc A. 1951;64:747–753.

[100] Cracknell A, Petch NJ. Frictional forces on dislocation arrays at the lower yield point in iron. Acta Metall. 1955;3:186–189.

[101] Cracknell A, Petch NJ. Frictional forces on dislocation arrays at the lower yield point in iron. Acta Metall. 1955;3(2):186–189.

[102] Honeycombe RWK. The plastic deformation of metals; 1968.

[103] Li JH, Dasgupta A. Failure-mechanism models for creep and creep rupture. IEEE Trans Reliab. 1993;42: 339–353.

[104] Maruyama K, Yamamoto R, Nakakuki H, et al. Effects of lamellar spacing, volume fraction and grain size on creep strength of fully lamellar tial alloys. Mater Sci Eng A. 1997;239:419–428.

[105] Shahinian P, Lane JR. Influence of grain size on high temperature properties of monel. Trans Am Soc Metal. 1953;45:177–199.

[106] Lee YS, Kim DW, Lee DY, et al. Effect of grain size on creep properties of type 316ln stainless steel. Metal Mater Int. 2001;7(2):107–114.

[107] Bhadeshia HKDH, Honeycombe RWK. Steels: micro structure and properties. 3rd ed. London: Butterworth-Heinemann; 2006.

[108] Thelning K. Steel and its heat treatment. Oxford: Butterworth-Heinemann; 2013.

[109] Karmakar A, Kundu S, Roy S, et al. Effect of microalloying elements on austenite grain growth in Nb–Ti and Nb–V steels. Mater Sci Technol. 2014;30(6):653–664.

[110] Hutchinson CR, Zurob HS, Sinclair CW, et al. The comparative effectiveness of Nb solute and NbC precipitates at impeding grain-boundary motion in Nb steels. Scr Mater. 2008;59:635–637.

[111] Kikuchi M, Sakakibara M, Otoguro Y. An austenitic heat resisting steel tube developed for advanced fossil steam plants. International Conference on Creep, p. 215–220, 1986.

[112] Adamson JM, Martin JW. Tertiary creep processes in 20 percent cr, 25 percent Ni austenitic stainless steels of differing nb/c ratios. Technical report, Oxford University, 1972.

[113] Keown SR, Pickering FB. Creep strength in steel and high temperature alloys. Metals Soc. 1972;210: 271–275.

[114] He XL, Djahazi M, Jonas JJ, et al. The non-equilibrium segregation of boron during the recrystallization of Nb-treated HSLA steels. Acta Metall Mater. 1991;39: 2295–2308.

[115] Tamehiro H, Murata M, Habu R, et al. Effect of combined addition of niobium and boron on thermomechanically processed steel. ISIJ Int. 1986;72:458–465.

[116] Porter DA, Easterling KE, Sherif M. Phase transformations in metals and alloys (revised reprint). CRC Press; 2009.